ELSEVIER

Nuclear Instruments and Methods in Physics Research A 435 (1999) 462–474

NUCLEAR INSTRUMENTS & METHODS IN PHYSICS RESEARCH Section A

www.elsevier.nl/locate/nima

Instrumental neutron activation analysis for studying size-fractionated aerosols

Imre Salma[a,*,1], Éva Zemplén-Papp[b]

[a]KFKI Atomic Energy Research Institute, H-1525 Budapest, P.O. Box 49, Hungary
[b]Chemistry Section of the Hungarian Academy of Sciences, H-1361 Budapest, P.O. Box 6, Hungary

Received 12 April 1999; received in revised form 28 May 1999; accepted 21 June 1999

Abstract

Instrumental neutron activation analysis (INAA) was utilized for studying aerosol samples collected into a coarse and a fine size fraction on Nuclepore polycarbonate membrane filters. As a result of the panoramic INAA, 49 elements were determined in an amount of about 200-400 μg of particulate matter by two irradiations and four γ-spectrometric measurements. The analytical calculations were performed by the absolute (k_0) standardization method. The calibration procedures, application protocol and the data evaluation process are described and discussed. They make it possible now to analyse a considerable number of samples, with assuring the quality of the results. As a means of demonstrating the system's analytical capabilities, the concentration ranges, median or mean atmospheric concentrations and detection limits are presented for an extensive series of aerosol samples collected within the framework of an urban air pollution study in Budapest. For most elements, the precision of the analysis was found to be beyond the uncertainty represented by the sampling techniques and sample variability.

PACS: 82.80.Jp; 82.70.Rr; 29.30.-h

Keywords: INAA, k_0 standardization; Size-fractionated aerosols; Elemental composition

1. Introduction

Aerosol particles in the air govern several basic atmospheric processes, and influence all terrestrial and aquatic ecosystems including the human health. Knowledge of the detailed chemical composition and physical characteristics of particulate matter is essential to our understanding of their behaviour and impact. The chemical composition of aerosols is exceedingly complex and, moreover, it is linked to particle size. Study of the elemental composition – and in particular the size-differentiated elemental composition – is of crucial importance because it is the inorganic components that are the major constituents of aerosols, and because it provides us with highly useful information on their sources and source processes.

Many analytical techniques have been utilized to investigate the environmental samples. These methods are described, discussed and compared in the literature, e.g., Refs. [1,2]. Generally speaking, instrumental neutron activation analysis (INAA)

* Corresponding author.
E-mail address: salma@para.chem.elte.hu (I. Salma)
[1] Present address: Department of Environmental Chemistry, L. Eötvös University, H-1518 Budapest 112, P.O. Box 32, Hungary.

0168-9002/99/$ - see front matter
PII: S0168-9002(99)00654-3

was found as the primary analytical technique for determining the elemental composition of the solid environmental samples. This is mainly so because its advantages, e.g., very little sample preparation or treatment, small amount of material needed, multi-element and non-destructive character, virtually no matrix effect, little matrix and collection substrate activation (low blank), high sensitivity and accuracy, etc., can be exploited very well in this field [3]. INAA's capabilities can further be extended by employing new developments in the standardization, and incorporating aspects of the recent progress in the nuclear measuring and data evaluation techniques [4–8]. At present, INAA utilizing absolute (k_0) standardization is considered to be the most advanced and optimized version of the method. Besides many undisputed benefits, its analysis protocol is possibly over-sophisticated, and extensive and the dedicated calibration and calculation procedures need to be performed before the applications. The main objectives of the present paper are to describe the experimental setup, to present the calibration and application procedures utilized, to report on the data reduction process developed, and to demonstrate the analytical achievements of the system established at the Budapest Research Reactor on a series of size-differentiated urban aerosol samples.

2. Collection of aerosol samples

As a part of a comprehensive air pollution study in Budapest, size-fractionated aerosol samples were collected by Gent-type stacked filter units (SFUs) [9]. The separation of the aerosol particles into two size fractions is achieved by the sequential filtration through two Nuclepore polycarbonate membrane filters of different pore size; each filter has a diameter of 47 mm. The first (coarse) and the second (fine) filters are placed in a stacked filter cassette that is equipped with an upper-size inlet cut-off. At a given airflow rate, the aerosol particles are separated into a coarse (about 10–2 μm equivalent aerodynamic diameter, EAD) and a fine (< 2 μm EAD) size fraction on the filters.

The aerosol samples were collected at three urban sites in Budapest [10,11]. With regard to the first two sites, one of them was chosen downtown in a small park at Széna Square at the automated monitoring station of the Municipal Institute of the State Public Health Officer Service (ÁNTSz FI). The second sampling site was located on the western border of Budapest within the wooded campus of the Central Research Institute for Physics (KFKI) of the Hungarian Academy of Sciences. Daily aerosol samples were taken with planned and regular interruptions at both places. The mean sampled volumes were 18.6 and 21.9 m^3, respectively. The sampling was performed consecutively from 9 April until 17 May 1996, and a total of 33 samples and 4 field blanks were collected at both sites. The field blanks are samples that were collected by carrying out all the same manipulations and operations as for real samples, even including drawing air through them for say 1 min. The third sampling site was downtown within the Castle District Tunnel, which is 350 m long, about 9 m wide and varies from 8 to 11 m in height. It comprises two-lane traffic of passenger cars, light-duty vehicles and buses. Two samples and a field blank were collected in the tunnel at about the halfway point from about 8 a.m. to 4 p.m. on 11 and 12 May 1998. The mean sampled volume was 5.6 m^3. All filters were placed into plastic Petri dishes and were stored in a refrigerator at a temperature of about 4°C.

3. Sample preparation and activation

Each filter was weighed before and after the sampling to obtain the particulate mass. The coarse and fine filters contained typically about 800 and 500 μg of particulate matter, respectively. The filters were then cut into sections. Usually, one-half of each SFU filter is investigated by INAA, a quarter section is analysed by particle-induced X-ray emission analysis (PIXE) [10,12], the remaining quarter is retained as a spare sample or for analysis by other techniques. If speciation analysis is to be performed by hyphenated techniques, three-quarter sections are employed, and one-quarter remains for determining the total elemental concentrations by INAA [11]. In this manner, the relative uncertainty introduced by cutting the filters and by analysing different portions is expected to be less

than 6% [13]. The filter sections intended for INAA were pressed into pellets with a diameter of 7 mm (standardized sample).

INAA of the pellets was performed in the Budapest Research Reactor. This is a tank-type reactor (VVRS-M), cooled and moderated by light water, and operated at a steady-state thermal power of 10 MW. The activation, measuring and decay scheme of INAA was optimized to the requirements of multi-element analysis, and is similar to that originally proposed in Ref. [14]. It consists of two activations: a short-time ($A1$) and a long-time ($A2$) neutron irradiation, and of two-spectrometric measurements ($M1$ and $M2$) after each activation. Each pellet was placed into a separate polyethylene vial (inner diameter 7 mm, inner height about 5 mm) and was irradiated individually by our vertical pneumatic transport facility. Coarse and fine filter sections were activated for 4 and 5 min, respectively. Each pellet was then transferred to another inactive polyethylene vial, and γ-spectrometry was performed. After a waiting time of at least two months, each pellet was placed in a separate high-purity synthetic quartz ampoule (Suprasil AN, inner diameter 7 mm, length about 45 mm) and sealed. The coarse and fine filter sections were irradiated separately (in bunches of 8 ampoules) in vertical irradiation channel 19 at position 2 for 14 and 16 h, respectively (long-time activation). After activation, the surface of the quartz ampoules was cleaned in an etching bath consisting of concentrated acids of HF, CH_3COOH and HNO_3 in a ratio of 20:20:60 vol.% for 2–3 min. The samples were measured together with the ampoules.

The subcadmium-to-epithermal neutron flux ratio ($f = \Phi_s/\Phi_e$) and the epithermal neutron flux shape factor (α) have to be measured only because of performing the analytical calculations by means of k_0 standardization [4]. The reactor operates according to a pre-determined timetable usually for 5, 10 or 14 d continuously with a shutdown period of 2 d or sometimes longer. After a certain time, the configuration of the active zone is also modified. The short-time irradiation runs (which took about 8 h a day) were always done on the 3rd day after the reactor was put into operation or later when the neutron spectrum could already be considered to be in the equilibrium state. Variation of f and α over one irradiation run was found to be within the standard deviation of the average value at the steady-state power of the reactor, so the parameters can be considered to be sufficiently constant. However, f and α vary from one irradiation run to another in this type of reactor. For routine INAA, the flux ratio and the shape factor should be determined for each irradiation run separately, preferably by in situ measurements (instantaneous monitoring). Within the concept of k_0 standardization, the bare triple monitor method is recommended for that purpose since this enables several neutron spectrum parameters to be calculated including f and α [15,16]. These parameters were determined (see later) at the beginning and at the end of each irradiation run, and the data obtained were intercompared, averaged and the mean values were used for that particular activation run in the analytical calculations. Time trends for f and α in the irradiation position of the pneumatic transport facility, together with the periods of shutdown and of different zone configurations are depicted in Fig. 1. It can be seen that f shows an increase, whereas α decreases when the zone configuration was not modified; it can also be seen that the parameters vary considerably in different configurations. (The biggest change during the experiments was found in epithermal neutron flux value, which increased by 30% when configuration No. 10 was changed to No. 11.) For the long-time activations, f and α values were determined for each irradiation, i.e., for each set of 8 ampoules irradiated together.

The triple monitor sets consisted of a thin multi-isotope Zr foil and an Au wire. A 4×4 mm piece of 100-μm thick high-purity (99.8%) Zr foil with a typical mass of about 5 mg served as the Zr monitor for the short-time activations, while a similar piece of high-purity (99.9%) Zr foil with a thickness of 25 μm and a mass of 1–2 mg was utilized in the long-time activations. The epithermal self-shielding factor for ^{94}Zr and ^{96}Zr in the 100-μm thick Zr foils was calculated analytically from the polynomial given in Ref. [4]; for the 25-μm thick Zr foils, the effect was neglected. The Zr monitor also offers the possibility for estimating the thermal neutron induced fission neutron flux (Φ_f) via the $^{90}Zr(n,2n)$

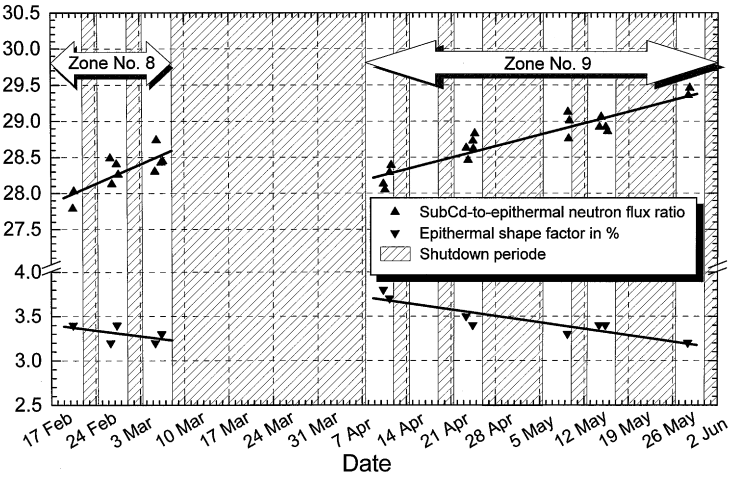

Fig. 1. Variation of subcadmium-to-epithermal neutron flux ratio (f) and epithermal neutron flux shape factor (α) in the irradiation position of the pneumatic transport facility over short-time INAA experiments.

^{89}Zr nuclear reaction, which is needed to correct for primary nuclear interference (see later). The Au monitor was used in dilute form as an Al–0.1% Au alloyed wire (IRMM-530) with a diameter of 0.5 mm and a mass of about 1 mg. The homogeneity and accuracy of the Au content of the wire were experimentally checked and approved [17]. The burn-up effect of the Au monitor in long-time activations was corrected for (by a typical factor of 0.98). The Zr–Au monitor set for the short-time activation was packed into a common polyethylene vial and was co-irradiated with the first and last sample of the irradiation runs. The Zr–Au monitor set for the long-time activation was wrapped in high-purity Al foil and co-irradiated with the bunch of 8 quartz ampoules in the central position. Occasionally, a 4×4 mm piece of 100-μm thick Fe foil with a mass of about 10 mg was added to the monitor sets for the long-time activations in order to check the consistency in both Φ_s and Φ_f determination via the ^{58}Fe(n, γ) ^{59}Fe and ^{54}Fe(n, p) ^{54}Mn nuclear reactions, respectively. All monitors were repacked after the activation. The Zr and Fe monitors were put into separate inactive polyethylene vials, the Au monitors were placed on the standardized sample holders for certified calibration point sources. Typical values of Φ_s, f, α and Φ_f for the irradiation position of the pneumatic transport facility over the irradiation runs were 5.4×10^{13} cm^{-2} s^{-1}, 28.6, 3.4% and 8×10^{12} cm^{-2} s^{-1}, respectively. If the polyethylene vial is properly positioned in the rabbit, less than 0.5% thermal neutron flux variation can be expected within the vials along the axis. Typical values of Φ_s, f, α and Φ_f for the vertical irradiation channel 19/2 over the irradiation runs were 1.7×10^{13} cm^{-2} s^{-1}, 38.7, 5.0% and 1.0×10^{12} cm^{-2} s^{-1}, respectively.

4. Calibration, measurement and data evaluation

The γ-ray spectrometer consists of a HPGe detector (relative efficiency 13%, FWHM = 1.74 at 1332.5 keV), and a spectroscopy amplifier CI 2020 (modified), analog-to-digital converter ND 583 (conversion gain 8k), loss-free counting system ND 583, and a high-voltage power supply CI 3125 all inserted into a NIM BIN power supply, and an Accuspec-B data acquisition board (resolution 2×8k) plugged into a personal computer. The loss-free counting module provides real-time compensation for different kinds of pulse losses, and corrects for variable counting rates and spectral shape [6]. This is of basic importance for measuring short-lived radionuclides. The loss-free counting module was fine-tuned by adjusting the pulse

evaluation time [18]. The accuracy of the correction as measured by the double-source (i.e., ^{60}Co and ^{137}Cs) method is within 1% up to an incoming counting rate of 50–60 kHz.

The absolute full-energy peak efficiency of the detector for the energy range from 60 keV up to 3.3 MeV was calibrated in sample-to-detector distances of 100, 50 and 20 mm (standardized geometries). Use was made of several certified absolute radioactivity standard point sources (i.e., ^{60}Co, ^{109}Cd, ^{134}Cs, ^{137}Cs, ^{133}Ba, ^{152}Eu and ^{241}Am) produced by the National Office for Measures (Hungary), and of some secondary multi-γ-ray calibration sources (i.e., ^{24}Na, ^{56}Mn, ^{56}Co, ^{75}Se, ^{82}Br, ^{110m}Ag, ^{140}La, ^{182}Ta and ^{192}Ir) [19]. The experimental efficiency data and the fitted orthogonal polynomial for a sample-to-detector distance of 100 mm are displayed in Fig. 2. Excellent precision was achieved: the relative standard deviation of the fitted efficiency curve remains within 1.2% in the energy range from 80 keV up to 3.1 MeV, and it is about 0.6% for the typical measuring range. Calibration of the full-width at half-maximum (FWHM) was performed by the same radioactivity standard point sources for amplification gains of 0.400 and 0.250 keV/ch. Calibration of the peak-to-total (P/T) ratio in the standardized geometries was accomplished by measuring some "coincidence-free" γ-ray point sources (e.g., ^{51}Cr, ^{57}Co , ^{65}Zn, ^{109}Cd, ^{137}Cs and ^{241}Am). As to energy calibration, the two-point external linear relationship was used as an initial approach. In order to improve the accuracy of energy determination, two appropriately located and statistically well developed and defined total energy peaks (usually ^{51}Ti: 320.08 keV and ^{24}Na: 2754.03 keV, or ^{153}Sm: 103.18 keV and ^{140}La: 1596.21 keV, or ^{82}Br: 221.50 and 1474.90 keV) were sought in the γ-ray spectra, and were utilized for establishing an individual internal linear energy calibration. To further refine the accuracy of the energy determination, the non-linearity curve of the entire measuring system was determined in advance by multi-γ-ray calibration sources at the same amplification gains as used for the samples. The non-linearity curve of the spectrometer recorded at an amplification gain of 0.250 keV/ch for an internal calibration by ^{82}Br radionuclide is exhibited in Fig. 3 as an example. The curves determined were utilized for correcting the non-linearity of the energy calibration in the γ-ray spectra of the samples. This approach enabled the energy of full-energy peaks with an area of about 5000 counts or more to be determined with an uncertainty of 0.1 keV even under routine measuring conditions. Most calibrations were performed using the quality assurance module of the Hypermet-PC computer program [8].

The samples were measured by a γ-spectrometer calibrated as described above. Two measurements

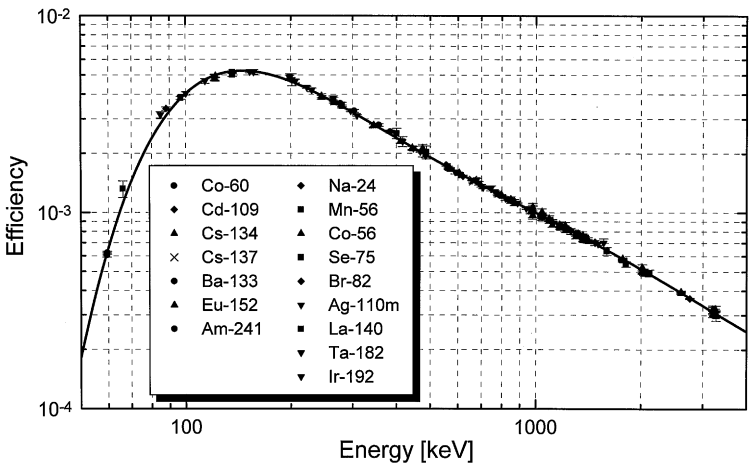

Fig. 2. Absolute full-energy peak efficiency curve of the detector for an energy range from 60 keV through 3.3 MeV at a sample-to-detector distance of 100 mm.

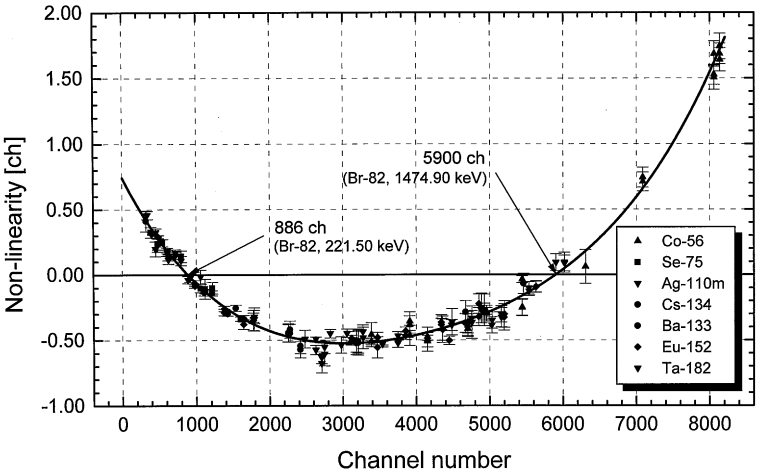

Fig. 3. Non-linearity curve of the entire measuring system at a resolution of 0.250 keV/channel for an internal two-point linear energy calibration at 221.5 and 1474.9 keV.

were performed after the short-time activation. The first one took place after a decay time of 1.5–6 min for a measuring time of 5 min, and the counting was repeated after a decay time of about 10 min for a measuring time of 30 min. Both measurements were accomplished at a sample-to-detector distance of 50 mm with an amplification gain of 0.400 keV/ch. After long-time activation, the pellets sealed in the quartz ampoules were measured after about 2 d of decay time for a measuring time of 2 h at a sample-to-detector distance of 100 mm, and again after about 6 d for 4–6 h at a sample-to-detector distance of 20 mm. These countings were accomplished with an amplification gain of 0.250 keV/ch in order to achieve the optimal energy resolution. The Zr monitors were measured after an average decay time of 2.8 d for a measuring time of 1.6 h (short-time activation) or for 40 min (long-time activation). Measurement of the Fe monitors took place after a decay time of about 14 d for about 1 h. The Au monitors were measured for about 40 min after a decay time of about 4 d (short-time activation) or 12 d (long-time activation). The monitors were measured in the highest standardized geometry. All γ-ray spectra were evaluated by the Hypermet-PC computer program [7]. This flexible spectrum analysis code handles even changes in full-energy peak shapes occurring when often a high incoming counting rate varies considerably from sample to sample and/or during one measurement. Special attention was paid to spectral interference; multiplets were deconvoluted satisfactorily or well.

A list of the elements detected, the analyte radionuclides with half-life and energy of analyte γ-rays utilized, and an overview of the activations/measurements are presented in Table 1. This table shows that 17 elements were determined by short-time INAA, while 36 elements were found by long-time INAA. Single or well resolved full-energy peaks (i.e., analyte γ-rays) only were utilized for quantification. The analytical calculations were performed in accordance with the k_0 standardization method following Høgdal's convention and including coincidence correction (reviewed in Ref. [4]), and the nuclear data needed for computations were taken from Ref. [5]. Elemental amounts were computed from all analyte γ-rays listed in Table 1. The weighted mean values, and the external (observed) and internal (expected) standard deviations for each element were derived for short- and long-time INAA separately. Comparison of the standard deviations was very useful for investigating the reliability of the individual concentration data. After the evaluations, the larger of the internal and external standard deviations was quoted as the uncertainty of the mean concentration. Mean blank values for Na, Al, Cl, V, Mn, Br

Table 1
Overview on elements determined by short-time (A1) and long-time (A2) activation followed by two γ-spectrometric measurements (M1 and M2) after each

Order No.	Element determined	Analyte radionuclide	Half-life	Energy [keV]	Measurement			
					A1M1	A1M2	A2M1	A2M2
1	Na	Na-24	14.91h	1368.6	•	•	•	•
				2754.0	•	•		
2	Mg	Mg-27	9.458 min	843.8	•			
				1014.4	•	•		
3	Al	Al-28	2.241 min	1778.9	•	•		
4	S	S-37	5.050 min	3103.4	•	•		
5	Cl	Cl-38	37.24 min	1642.7	•	•		
				2167.4	•	•		
6	K	K-42	12.36 h	1524.7		•	•	
7	Ca	Ca-49	8.718 min	3084.4	•	•		
		Ca-47	4.536 d	1297.1			•	•
		Sc-47	3.341 d	159.4				•
8	Sc	Sc-46	83.83 d	889.3				•
				1120.5				•
9	Ti	Ti-51	5.760 min	320.1	•	•		
10	V	V-52	3.743 min	1434.1	•	•		
11	Cr	Cr-51	27.70 d	320.1			•	•
12	Mn	Mn-56	2.578 h	846.8		•		
				1810.7	•	•		
				2113.1	•	•		
13	Fe	Fe-59	44.50 d	1099.3			•	•
				1291.6			•	•
14	Co	Co-60	5.271 y	1332.5				•
15	Cu	Cu-66	5.088 min	1039.2	•	•		
16	Zn	Zn-69m	13.76 h	438.6			•	
		Zn-65	244.1 d	1115.5				•
17	Ga	Ga-72	14.10 h	630.0			•	
				834.0			•	
18	As	As-76	1.097 d	559.1			•	
				657.1			•	
19	Se	Se-75	119.8 d	136.0				•
				264.7				•
20	Br	Br-82	1.471 d	554.3	•	•	•	•
				619.1			•	•
				698.4		•	•	•
				776.5		•	•	•
				827.8		•	•	•
				1044.0		•	•	•
				1317.5		•	•	•
				1474.9		•	•	•
21	Rb	Rb-86	18.66 d	1077.0				•
22	Sr	Sr-87m	2.795 h	388.5		•		
23	Mo	Mo-99	2.748 d	140.5			•	•
24	Ru	Ru-97	2.88 d	215.7				•
25	Ag	Ag-110m	249.8 d	657.8				•
				884.7				•
				937.5				•

(Cont.)

Table 1 *continued*

Order No.	Element determined	Analyte radionuclide	Half-life	Energy [keV]	Measurement			
					A1M1	A1M2	A2M1	A2M2
26	Cd	In-115m	4.486 h	336.2				•
		Cd-115	2.228 d	527.9				•
27	In	In-116m	54.41 min	1097.3		•		
				1293.5		•		
28	Sb	Sb-122	2.70 d	564.2			•	•
				692.7			•	•
		Sb-124	60.20 d	602.7				•
				645.9				•
				722.8				•
				1691.0				•
29	Te	I-131	8.040 d	364.5				•
30	I	I-128	24.99 min	442.9		•		•
31	Cs	Cs-134	2.062 y	604.7				
				795.9				•
32	Ba	Ba-139	1.380 h	165.9	•	•		
		Ba-131	11.5 d	123.8				•
				216.1				•
				496.3				•
33	La	La-140	1.678 d	328.8				•
				487.0			•	•
				815.8			•	•
				1596.2			•	•
34	Ce	Ce-141	32.50 d	145.4				•
35	Sm	Sm-153	1.946 d	103.2			•	•
36	Eu	Eu-152!	13.33 y	344.3				•
				867.4				•
				964.1				•
37	Dy	Dy-165	2.334 h	94.7		•		
				361.7	•			
38	Yb	Yb-175	4.19 d	113.8				•
				282.5				•
				396.3				•
39	Lu	Lu-177!	6.71 d	208.4				•
40	Hf	Hf-181	42.39 d	133.0				•
				482.2				•
41	Ta	Ta-182	115.0 d	152.4				•
				222.1				•
				1121.3				•
				1189.1				•
42	W	W-187	23.9 h	479.6			•	•
				685.7			•	•
43	Re	Re-186	3.777 d	137.2				•
44	Ir	Ir-194	19.15 h	293.5			•	•
				328.4			•	•
45	Pt	Au-199	3.139 d	158.4				•
46	Au	Au-198	2.694 d	411.8			•	•
47	Hg	Hg-203	46.6 d	279.2				•
48	Th	a-233	27.0 d	312.2				•
49	U	Np-239	2.355 d	228.1			•	•
				277.6			•	•

• Means that the analyte γ-ray was in general detected in that particular measurement

and I for short-time INAA were also calculated for coarse and fine filters separately from all field blank filters. Similarly, mean blank values for Na, K, Cr, coarse Co, Ga, fine As, Br, Mo, coarse Sb, coarse La, W and Au for long-time INAA were calculated for coarse and fine filters separately from all field blank filters. The relative standard deviation of the mean blank values was less than 15–20%. The mean blank values were subtracted from the corresponding mean elemental amounts, and atmospheric concentrations (in ng/m^3) were derived. The mean concentrations obtained from the short- and long-time INAA were compared and then combined into common data sets. The Si concentration in the samples was obtained by PIXE with good precision [10], and it was used to correct the primary nuclear interference of ^{28}Al from the ^{28}Si(n, p) nuclear reaction. The corrected Al concentration was used further to account for the primary nuclear interferences of ^{24}Na from ^{27}Al(n, α), and of ^{27}Mg from ^{27}Al(n, p) reactions. The apparent atmospheric concentration $C(X)$ of an interfered element $X(=$ Al, Na or Mg) in ng/m^3 simulated by the interfering element $Y(=$ Si, Al and Al, respectively) present in an atmospheric concentration of $C(Y)$ in ng/m^3 due to its fast neutron reaction was calculated [20,21]

$$C(X) = \frac{A_{\mathrm{sp,\,Zr89}}}{A_{\mathrm{sp,\,Zr95}}} \cdot \frac{k_{0,\,\mathrm{Au}}(\mathrm{Zr94})}{k_{0,\,\mathrm{Au}}(X)} \cdot \frac{f + Q_{0,\,\mathrm{Zr94}}(\alpha)}{f + Q_{0,\,X}(\alpha)} \cdot \frac{\varepsilon(\mathrm{Zr95})}{\varepsilon(\mathrm{Zr89})} \times \frac{\bar{\sigma}(Y)\theta(Y)\,\gamma\,(Y)/A(Y)}{\bar{\sigma}(\mathrm{Zr90})\,\theta\,(\mathrm{Zr90})\,\gamma\,(\mathrm{Zr89})/A(\mathrm{Zr})} C(Y).$$

$A_{\mathrm{SP},i}$ is the specific full-energy peak count rate of the analyte γ-ray of radionuclide i, $k_{0,\,\mathrm{Au}}(i)$ is the k_0 factor of the analyte γ-ray and of the analyte stable nuclide i with respect to ^{198}Au, f is the subcadmium-to-epithermal neutron flux ratio, $Q_{0,i}(\alpha)$ is the cross section ratio of radionuclide i corrected for α, $\varepsilon(i)$ is the absolute full-energy peak efficiency for the analyte γ-ray of radionuclide i, $\sigma(i)$ the microscopic activation cross section of the analyte stable nuclide i averaged for the thermal neutron-induced fission spectrum of ^{235}U, $\Theta(i)$ is the isotope abundance of nuclide i or of the analyte stable nuclide of element i, $\gamma(i)$ is the absolute intensity of the analyte γ-ray from nuclide i, and $A(i)$ is the atomic number of element i. The interference correction factors were also determined experimentally by irradiating pieces of high-purity Si wafer, and of high-purity Al foils together with the neutron spectrum monitor sets. Good agreement was found between the calculated and measured interference factors. The apparent concentrations due to nuclear interference were subtracted from the corresponding data. The atmospheric concentration of Al, Na and Mg was typically decreased with the correction by about 1%, 0.1% and 15–28%, respectively. The primary nuclear interferences become in general less important for elements with large atomic numbers and, therefore, the perturbation effect of other primary nuclear interference on the aerosol analysis was neglected. Nuclear interferences of ^{99}Mo, ^{140}La and ^{141}Ce from ^{235}U(n, f) were also corrected for when the U concentration made it necessary. The apparent atmospheric concentration $C(X)$ of an interfered element $X(=$ Mo, La or Ce) in ng/m^3 simulated by the uranium that is present in an atmospheric concentration of $C(U)$ in ng/m^3 by virtue of its fission was calculated as [20]

$$C(X) = \frac{A(X)}{A(U)} \frac{\theta(U235)}{A(X)} \frac{\sigma_{0,\,\mathrm{fiss}}\, f + Q_{0,\,\mathrm{fiss}}(\alpha)}{\sigma_{0,\,X}\; f + Q_{0,\,X}(\alpha)} w_X C(U)$$

where w_X is the cumulative fission yield of the analyte radionuclide, σ_0 is the microscopic cross section at 2200 m/s neutron velocity for (n, γ) activation or fission reaction. The analyte fission product has to have a much longer half-life than any of its precursors in the isobaric decay chain otherwise appropriate corrections for multiple radioactive transitions need to be adopted. The atmospheric concentration of Mo, La and Ce was typically decreased with the correction by about 5–8%, 0.5% and 2–3%, respectively in the coarse size fraction.

5. Results and discussion

As a consequence of the measuring and data reduction systems described, INAA involves an internal consistency. The concentration of many elements was computed from several analyte γ-rays of (sometimes very) different energies. In addition,

some elements, viz., Na, K, Ca, Br and Ba were generally measured after both short- and long-time activations. Their intermediate concentrations were affected by dissimilar neutron spectrum and other activation parameters, by measurements in the different standardized geometries calibrated separately, by counting under very diverse measuring conditions and setup, and by applying discrepant blank and other corrections. The ratio of concentrations obtained by the short- and long-time activations was employed for continuous quality control of the procedure. Moreover, some elements, i.e., Ca and Ba (and from a certain point of view Zn, Cd and Sb as well) were determined via distinct radionuclides. Agreement between their intermediate concentration values also provides support for the validity of the analytical technique. Average concentration ratios for the short- and long-time INAA are given in Table 2. Quality assurance of the concentration data, in particular in connection with the PIXE results, is to be dealt with in detail in a separate article.

Table 1 shows that 49 elements were determined in the aerosol samples. However, for a few elements detection limits only were obtained for almost all samples and, therefore, derived data that were representative and meaningful for the whole series were obtained for a decreased number of elements. Results of the panoramic INAA for the coarse and fine fractions are displayed in Tables 3 and 4, respectively. The tables report median or mean atmospheric concentrations. Mean values are given when the number of concentration data was less than half the number of samples. Note that the detection limits were set equal to zero when calculating the medians, but were left out when calculating the means. The median or average atmospheric concentrations cover 6–7 orders of magnitude (from pg/m^3 through $\mu g/m^3$). From systematic comparison of the internal and external standard deviations, it turned out that in most cases, the precision was governed by the counting statistics. In general, Na, coarse Mg, Al, Cl, K, coarse Sc, V, Mn, Fe, Zn, As, Br, Sb, fine I, La and Sm were determined with a relative uncertainty below 5%, and fine Mg, Ca, fine Sc, coarse Ti, Cr, coarse Co, Cu, Ba, coarse Ce, Dy, W, and Au were determined with a relative uncertainty between 5 and about 10%, while S, fine Ti, fine Co, Ga, Se, Sr, Mo, Ru, In, coarse I, fine Ce, Eu, Yb, Lu, Hf, Hg, Th and U were determined with a relative uncertainty between 10 and about 20%. Bearing in mind the small amount of particulate matter analysed, it is most likely that the sampling technique, the sample variability and inhomogeneity, and the volumetric uncertainty of the sampled air have a much higher contribution to the random error of most concentrations than the analysis itself. It should be mentioned that the concentrations of Eu and Lu need to be approached with a certain amount of caution in that they were determined on the basis of Høgdal's convention via radionuclides whose activation cross sections do not obey the $1/v$ law. The estimated analytical error for these elements due to the simplified convention is still below their experimental uncertainty [4].

Table 2
Average ratio of concentrations ($A1/A2$) obtained by short-time ($A1$) and long-time ($A2$) INAA, and its standard deviation [$s(A1/A2)$]

Element	$A1/A2$	$s(A1/A2)$
Na	1.02	0.05
K	1.02	0.06
Ca	0.94	0.10
Br	1.00	0.09
Ba	0.98	0.10

Detection limits were determined for coarse and fine size fractions separately, and some of them are also presented in Tables 3 and 4, respectively. For elements that were present in the blank filters, the variability of the blank was mostly the limiting factor of the detection limits. The net amount (after blank correction) in a real sample was always compared with the standard deviation of the mean blank value (s_{blank}). When the net amount was less than $3s_{blank}$, a detection limit was calculated, and it was set at $3s_{blank}$ value. For elements that were not present in the blank filters, the detection limits strongly depend on the presence of other elements in the sample (in particular Na and Br have deterioration effects), and – hence – vary from sample to sample. The minimal values for the detection limits were found for the filters with least aerosol mass,

Table 3
Detection limit, number of concentration data (No.), concentration range, median or mean atmospheric concentration (all in ng/m^3) for coarse aerosol samples collected at Széna Square, KFKI campus, and within the Castle District Tunnel - all in Budapest

Element	Detection limit	Széna Square			KFKI campus			CD Tunnel	
		No.	Range	Median	No.	Range	Median	No.	Mean
Na	0.94	33	122–673	311	33	14–236	84	2	1043
Mg	8.7	33	182–994	512	33	25–380	131	2	2230
Al	0.88	33	431–2183	1294	33	43–990	334	2	4387
Cl	3.3	33	65–582	166	32	11–144	48	2	903
K	4.0	33	127–768	429	33	33–314	140	2	1687
Ca	3.9	33	920–4453	2430	33	69–1459	447	2	12309
Sc	0.0029	33	0.08–0.41	0.24	33	0.01–0.20	0.063	2	0.92
Ti	4.9	33	37–157	89	31	6–62	24	2	411
V	0.033	33	1.1–6.9	3.2	33	0.2–2.6	1.0	2	12
Cr	13	0	$<14-<28$	–	0	$<13-<19$	–	1	58
Mn	0.033	33	10–52	31	33	1.3–17.5	5.9	2	191
Fe	25	33	669–3025	1914	31	40–838	275	2	15545
Co	0.055	29	0.18–1.14	0.42	11	0.14–0.37	0.22[a]	2	1.8
Cu	5.2	33	15–59	34	2	10–14	12[a]	2	738
Zn	1.4	33	18–165	55	31	3–22	11	2	571
Ga	0.060	24	0.15–1.16	0.59	23	0.06–0.59	0.26	0	–
As	0.059	33	0.4–3.1	1.3	30	0.11–1.63	0.46	2	4.5
Br	2.1	33	4–25	12	14	2.5–4.6	3.2[a]	2	529
Sr	4.5	8	9–19	14[a]	3	4.5–6.6	5.7[a]	1	83
Mo	0.17	33	0.5–3.4	1.0	10	0.17–0.33	0.20[a]	2	41
Ru	0.60	10	1.9–5.2	3.7[a]	2	1.1–1.3	1.2[a]	0	–
In	0.0030	13	0.0037–0.0114	0.0079[a]	9	0.0034–0.0055	0.0044[a]	0	–
Sb	0.017	33	2.0–9.5	6.0	33	0.02–0.93	0.16	2	196
I	0.090	29	0.13–1.42	0.46	32	0.09–1.52	0.29	2	3.7
Cs	0.046	0	$<0.15-<0.50$	–	5	0.06–0.15	0.12[a]	0	–
Ba	1.0	33	14–53	35	24	1.1–11.8	5.5	2	547
La	0.030	33	0.23–1.30	0.71	33	0.03–0.54	0.20	2	2.8
Ce	0.16	33	0.6–3.1	1.5	27	0.16–1.29	0.61	2	10
Sm	0.0031	33	0.03–0.19	0.11	33	0.003–0.091	0.034	2	0.43
Eu	0.0030	15	0.011–0.080	0.036[a]	0	$<0.03-<0.04$	-	0	–
Dy	0.004	28	0.06–0.30	0.11	25	0.017–0.108	0.048	2	0.35
Yb	0.023	11	0.02 7–0.081	0.058[a]	3	0.023–0.030	0.027[a]	0	–
Lu	0.0030	18	0.014–0.029	0.023	9	0.009–0.014	0.011[a]	0	–
Hf	0.033	11	0.06–0.22	0.16[a]	1	–	0.041	2	1.2
W	0.062	25	0.16–1.29	0.33	8	0.14–0.23	0.20[a]	1	–
Au	0.0005	27	0.0013–0.0300	0.0028	8	0.0014–0.0127	0.0045[a]	2	0.013
Th	0.027	29	0.09–0.45	0.24	14	0.05–0.17	0.12[a]	1	0.84
U	0.040	20	0.04–0.50	0.10	9	0.08–0.13	0.11[a]	0	–

[a]Represents mean.

i.e., for some field blanks after blank correction and assuming the average sampled volume. Nevertheless, detection limits for these elements turn out to be more realistic when they are calculated according to the L_D criterion of Currie [22]. The background under the full-energy peak was always integrated over a $3 \cdot \mathrm{FWHM}$ region, where the actual FWHM was obtained from FWHM calibration. These calculations resulted in a series of detection limits for each element. The minimal value in the series was considered to be the representative detection limit. For most elements,

Table 4
Detection limit, number of concentration data (No.), concentration range, median or mean atmospheric concentration (all in ng/m^3) for fine aerosol samples collected at Széna Square, KFKI campus, and within the Castle District Tunnel – all in Budapest

Element	Detection limit	Széna Square			KFKI campus			CD Tunnel	
		No.	Range	Median	No.	Range	Median	No.	Mean
Na	1.5	33	27–109	52	33	13–101	50	2	40
Mg	5.7	33	24–107	52	32	7–13	31	2	73
Al	0.68	33	47–245	116	33	12–367	87	2	124
S	457	10	1683–3645	2375[a]	20	1385–3136	2204	0	–
Cl	5.6	29	10–63	21	25	9–63	18	2	73
K	3.5	33	43–274	131	33	27–318	150	1	126
Ca	2.8	33	67–372	186	31	26–319	93	2	354
Sc	0.0024	33	0.011–0.047	0.024	30	0.007–0.066	0.020	1	0.061
Ti	2.9	26	6–18	11	27	4.1–22.6	7.6	0	–
V	0.018	33	0.5–3.4	1.6	33	0.7–5.8	1.8	2	1.3
Cr	1.5	30	1.6–9.2	3.1	11	1.5–7.0	2.8[a]	0	–
Mn	0.011	33	2.5–19.8	7.0	33	0.5–11.0	4.0	2	9.5
Fe	22	33	108–510	343	31	18–249	122	2	897
Co	0.037	33	0.11–0.62	0.23	33	0.05–0.43	0.12	0	–
Cu	0.9	33	5–21	11	24	0.9–6.7	3.1	2	54
Zn	1.4	33	13–91	35	33	4–58	21	2	59
Ga	0.058	29	0.07–0.67	0.17	18	0.07–0.53	0.19	0	–
As	0.039	33	0.2–4.3	1.2	33	0.1–3.5	1.0	1	0.64
Se	0.31	16	0.49–2.28	0.99[a]	30	0.33–1.96	0.67	0	–
Br	0.96	33	6–24	15	33	1.5–9.0	5.0	2	141
Rb	0.8	2	1.6–2.1	1.8[a]	3	0.8–1.4	1.0[a]	0	–
Mo	0.11	26	0.23–1.16	0.43	15	0.12–0.61	0.24[a]	2	3.5
Cd	0.45	0	$< 0.9 - < 1.5$	–	13	0.45–1.44	0.91[a]	0	–
In	0.0015	27	0.0016–0.0962	0.0040	27	0.0015–0.0147	0.0043	0	–
Sb	0.027	33	1.4–7.0	2.3	33	0.13–3.90	0.61	2	11
I	0.14	33	0.5–2.4	1.1	33	0.8–4.1	2.0	2	7.0
Cs	0.033	4	0.061–0.116	0.079[a]	13	0.06–0.25	0.12[a]	0	–
Ba	1.2	33	3.5–10.4	7.7	12	1.2–3.9	2.6[a]	2	33
La	0.012	33	0.05–0.22	0.11	32	0.020–0.260	0.077	2	0.19
Ce	0.15	16	0.19–0.56	0.37[a]	27	0.15–0.58	0.25	0	–
Sm	0.0018	33	0.005–0.022	0.012	31	0.0025–0.0341	0.0093	1	0.029
W	0.045	20	0.18–6.54	0.22	12	0.17–1.88	0.90[a]	1	4.9
Au	0.00065	5	0.0013–0.0055	0.0030[a]	4	0.0012–0.0017	0.0055[a]	2	0.019
Hg	0.12	13	0.13–0.37	0.24[a]	31	0.19–1.03	0.37	0	–

[a] Represents mean.

however, the measured concentrations exceeded the detection limits considerably, which had a beneficial influence on the precision of the determination. Interestingly, Pt which is said to be emitted from the catalytic converters of vehicles driven by petrol engines was virtually not detected in the urban aerosol, and its concentration was below the detection limit of about 0.6 and 0.4 ng/m^3 for coarse and fine size fractions, respectively.

The atmospheric concentrations obtained by INAA will be combined with the independent data obtained by PIXE, and will be complemented by the results of other analytical techniques, by concentrations of some criteria pollutants, and by meteorological data. The ultimate data sets for the size fractions and the sampling sites are to be used for determining the chemical and temporal characteristics of urban aerosols in Budapest and for receptor modelling calculations. The interpretation of the analytical and modelling results and their conclusions are being prepared for separate publication.

Acknowledgements

This work was funded by the Hungarian Scientific Research Fund (OTKA) under contract No. F014962. The assistance of J. Márton and B. Kálmán in the irradiation of samples is gratefully acknowledged.

References

[1] W. Maenhaut, Analytical Techniques for Atmospheric Trace Elements, in: J.M. Pacyna, B. Ottar (Eds.), Control and Fate of Atmospheric Trace Metals, Kluwer, Dordrecht, 1989.
[2] B. Sansoni, Multi-Element Analysis for Environmental Characterization and its Future Trends, Kernforschungsanlage, No. 393, Jülich, Germany, 1987.
[3] R. Dams, Pure and Appl. Chem. 64 (1992) 991.
[4] F. De Corte, The k_0 Standardization Method, Thesis, University of Gent, Gent, Belgium, 1987.
[5] F. De Corte, A. Simonits, J. Radioanal. Nucl. Chem. 133 (1989) 43.
[6] G.P. Westphal, J. Radioanal. Nucl. Chem. 114 (1987) 257.
[7] B. Fazekas, G. Molnár, T. Belgya, L. Dabolczi, A. Simonits, J. Radioanal. Nucl. Chem. 215 (1997) 271.
[8] B. Fazekas, J. Östör, Z. Kiss, A. Simonits, G.L. Molnár, J. Radioanal. Nucl. Chem. 233 (1998) 101.
[9] W. Maenhaut, F. François, J. Cafmeyer, The "Gent" stacked filter unit sampler for the collection of atmospheric aerosols in two size fractions, in: Applied Research on Air Pollution Using Nuclear-related Analytical Techniques, Report NAHRES-19, International Atomic Energy Agency, Vienna, Austria, 1994.
[10] I. Salma, W. Maenhaut, É. Zemplén-Papp, J. Bobvos, Microchem. J. 58 (1998) 291.
[11] Z. Šlejkovec, I. Salma, J.T. van Elteren, É. Zemplén-Papp, Fres. J. Anal. Chem. (1999) submitted for publication.
[12] I. Salma, W. Maenhaut, H.J. Annegarn, M.O. Andreae, F.X. Meixner, M. Garstang, J. Radioanal. Nucl. Chem. 216 (1997) 143.
[13] R. Heindryckx, R. Dams, Bull. Soc. Chim. Belg. 82 (1973) 611.
[14] R. Dams, J.A. Robbins, K.A. Rahn, J.W. Winchester, Anal. Chem. 42 (1970) 861.
[15] A. Simonits, F. De Corte, J. Hoste, J. Radioanal. Chem. 31 (1976) 467.
[16] F. De Corte, K. Sordo-El Hammami, L. Moens, A. Simonits, A. De Wispelaere, J. Hoste, J. Radioanal. Chem. 62 (1981) 209.
[17] J. Kucera, A. Simonits, F. De Corte, F. Bellemans, Proceedings of the second International k_0 Users Workshop, Ljubljana, Slovenia, 1997.
[18] S. Pommè, J.-P. Alzetta, J. Uyttenhove, B. Denecke, G. Arana, P. Robouch, Nucl. Instr. Meth. A 422 (1999) 388.
[19] X-ray and γ-ray Standards for Detector Calibration, TEC-DOC-619, International Atomic Energy Agency, Vienna, Austria, 1991.
[20] L. Xilei, D. Van Renterghem, F. De Corte, R. Cornelis, J. Radioanal. Nucl. Chem. 133 (1989) 153.
[21] Handbook on Nuclear Activation Cross-Sections, Technical Report Series No. 156, International Atomic Energy Agency, Vienna, Austria, 1974.
[22] L.A. Currie, Anal. Chem. 40 (1968) 587.